Journal of Architectural and Planning Research
37:4 (Winter, 2023) 55

MINERALOGICAL PREDICTORS OF VOLCANIC-ADDITIVE RESPONSIVENESS IN LIGHTWEIGHT AGGREGATES: COMPARATIVE EFFECT-SIZE EVIDENCE FROM TEN EXPANDABLE CLAYS

Zora Goodwin Jr.

Volcanic additives are increasingly considered as low-cost modifiers for lightweight aggregate (LWA) production, yet their effectiveness is strongly deposit-dependent. The unresolved question is not whether perlite and rhyolite tuff can improve bloating behavior, but which raw-clay characteristics determine when those improvements occur simultaneously in expansion, density reduction, and strength development. This study re-examines a ten-clay experimental matrix from Hungary and Egypt in which $10\,\mathrm{wt\%}$ *perlite or rhyolite tuff was incorporated into expandable clays and the resulting maximum height expansion (MHE), bulk density (BD), uniaxial compressive strength (UCS), and fired amorphous content were measured. A response-oriented analytical framework was used, combining outcome-specific effect sizes, a transparent composite benefit score, Spearman rank correlations, paired non-parametric tests, threshold-based classification, and robustness checks based on additive-specific subsets and clay-level aggregation. Quartz-rich, low-kaolinite clays were consistently more responsive than kaolinite-rich clays. Across 20 additive-treated observations, raw quartz correlated positively with the composite benefit score (*$\rho = 0.773$, $p < 0.001$*), whereas kaolinite correlated negatively (*$\rho = -0.655$, $p = 0.002$*). Density improvement was the most mineralogically sensitive outcome, tracking raw quartz (*$\rho = -0.728$, $p < 0.001$*) and kaolinite (*$\rho = 0.498$, $p = 0.025$*). All eight additive-treated observations with a quartz/kaolinite ratio greater than 1 achieved concurrent improvement in MHE, BD, and UCS, compared with only 2 of 12 observations at or below that threshold (Fisher exact* $p = 0.0007$*). The same ranking pattern remained directionally consistent when responses were examined separately for perlite and tuff and when they were averaged to one observation per clay. Perlite and tuff did not differ significantly in paired comparisons, indicating that raw clay mineralogy exerts a stronger control than additive identity at the selected dosage. The results support a practical mineralogical screening heuristic for additive selection before pilot firing and clarify the process–structure–property pathway linking raw mineralogy, glass-phase development, and final LWA performance, while also indicating the need for broader validation across additional deposits and firing schedules.*

https://doi.org/10.66033/japr2022-405

INTRODUCTION

Lightweight aggregates (LWAs) remain a strategically important constituent of structural and non-structural lightweight concretes because they reduce dead load while improving thermal performance and transport economy (Hossain, 2004; Rashad, 2018). Artificial LWAs produced from expandable clays are especially attractive because bloating, shell formation, and pore development can be tuned through raw-material selection and thermal processing (Huang & Liao, 2011; Hung & Hwang, 2007; Riley, 1951). At the same time, the central design challenge persists: lower density is desirable, but excessive porosity or unstable shell development can compromise mechanical resistance.

Volcanic materials such as zeolitic tuffs and perlite have received considerable attention in cementitious systems and lightweight concrete owing to their silica-rich character, low density, and broad availability (Dondi et al., 2004; Pekgöz & Tekin, 2021). A parallel line of work has shown that additives introduced directly into clay feedstocks can alter gas generation, viscosity windows, sintering temperature, pore architecture, and crushing resistance (Bernhardt et al., 2014; Soltan et al., 2016; Wei et al., 2018). However, most studies still evaluate additive performance in a deposit-specific way, reporting whether a given modifier improved a given clay, rather than identifying the mineralogical conditions under which improvement is likely.

A recent ten-clay experimental program by Abdelfattah et al. (2023) provides a strong basis for addressing that gap. In that study, ten expandable clays from Hungary and Egypt were characterized by X-ray fluorescence (XRF), X-ray diffraction (XRD/Rietveld), heating microscopy, firing tests, density testing, compressive strength testing, and microstructural examination. Perlite and rhyolite tuff were each added at 0, 5, 10, and 20 wt%, and 10 wt% was identified as the most favorable dosage overall. The study demonstrated that both additives can improve bloating and, in selected cases, yield aggregates with lower density and higher strength (Abdelfattah et al., 2023). It also showed that fired amorphous content is inversely related to density. What it did not formalize, however, is why some clays benefit strongly while others show neutral or adverse responses under the same additive dosage, nor whether a simple mineralogical screen could identify such cases in advance.

That unresolved heterogeneity is not a minor detail; it is the key scientific and industrial question. If additive responsiveness is governed by raw mineralogy, then simple pre-screening metrics could reduce unnecessary pilot firing, improve raw-material allocation, and support lower-risk scale-up. The present study therefore re-interrogates the same ten-clay experimental matrix through a moderator-oriented lens. The contribution is not a new additive, firing route, or raw-material library, but a more explicit decision framework for extracting predictive information from an already well-characterized experimental dataset. The specific aims are to:

1. quantify additive responsiveness using explicit effect-size metrics for expansion, density, and strength;
2. identify which raw-clay descriptors most strongly predict favorable multi-criteria response;
3. test whether a simple quartz/kaolinite-based screening index can separate full-response and mixed-response behavior; and
4. connect raw mineralogical selection to the downstream glass-phase–density relationship reported in the original experimental program.

By focusing on *conditional effectiveness* rather than average additive benefit, the manuscript advances a distinct contribution: an exploratory mineralogical selection framework for volcanic-additive use in LWA manufacture. Throughout, the results are interpreted as a screening-oriented secondary analysis of a published experimental matrix, rather than as a fully validated universal prediction model.

MATERIALS AND ANALYTICAL FRAMEWORK

Experimental matrix

The analysis uses the ten-clay experimental matrix reported by Abdelfattah et al. (2023). The raw materials comprised three Hungarian Pannonian clays (B, Y, G) and seven Egyptian clays (GZ1, FA2, SN3, HL4, HL5, SA6, SA7). Perlite and rhyolite tuff from the Zemplén Mountains were used as volcanic additives. Raw clays were characterized by XRF and XRD/Rietveld; bloating behavior was measured by heating microscopy; pellets were fired at six temperatures between 1150 °C and 1275 °C; and the fired products were characterized by bulk density, uniaxial compressive strength, mineral phase composition, and microscopy (Abdelfattah et al., 2023). The original study identified 10 wt% additive as the most effective dosage overall and reported final aggregate properties at 1225 °C for Hungarian clays and 1275 °C for Egyptian clays (Abdelfattah et al., 2023).

Table 1 lists the raw descriptors used in the present analysis. The Hungarian clays were quartz-rich and kaolinite-poor, whereas the Egyptian clays had substantially higher kaolinite contents, consistent with the geological background described for the source deposits (Abdelfattah et al., 2023; Agha et al., 2012; Gaber & Hassanien, 2011).

Table 1: Key raw-clay descriptors used as candidate moderators of additive responsiveness, assembled from the experimental matrix reported by Abdelfattah et al. (2023).

Sample	Origin	Quartz (wt%)	Kaolinite (wt%)	Flux (wt%)	Raw amorphous (wt%)	Quartz/kaolinite
B	Hungary	26.53	2.57	19.31	9.00	10.32
Y	Hungary	32.50	1.68	17.43	11.99	19.35
G	Hungary	30.80	3.20	18.34	6.10	9.62
GZ1	Egypt	11.35	27.23	21.24	10.00	0.42
FA2	Egypt	19.23	18.35	17.53	7.00	1.05
SN3	Egypt	22.01	22.87	16.75	6.20	0.96
HL4	Egypt	14.44	21.74	16.90	9.98	0.66
HL5	Egypt	6.27	34.00	16.76	10.00	0.18
SA6	Egypt	2.99	33.46	20.04	9.10	0.09
SA7	Egypt	3.96	33.30	19.60	6.10	0.12

Flux denotes the sum of Fe_2O_3 + MgO + CaO + Na_2O + K_2O, following the source study.

Derived response metrics

The present work evaluates additive responsiveness at the 10 wt% dosage using three outcome-specific effect sizes:

$$\Delta\mathrm{MHE}_{i,a} = \mathrm{MHE}_{i,a} - \mathrm{MHE}_{i,0}, \tag{1}$$

$$\Delta\mathrm{BD}_{i,a} = \mathrm{BD}_{i,a} - \mathrm{BD}_{i,0}, \tag{2}$$

$$\Delta\mathrm{UCS}_{i,a} = \mathrm{UCS}_{i,a} - \mathrm{UCS}_{i,0}, \tag{3}$$

where i denotes the clay sample, a denotes the additive (perlite or tuff), and the subscript 0 refers to the additive-free control.

Positive ΔMHE and ΔUCS indicate beneficial change, whereas negative ΔBD indicates beneficial density reduction. To summarize multi-criteria performance in a transparent way, a composite benefit score S was defined as

$$S_{i,a} = I(\Delta\mathrm{MHE}_{i,a} > 0) + I(\Delta\mathrm{BD}_{i,a} < 0) + I(\Delta\mathrm{UCS}_{i,a} > 0), \tag{4}$$

where $I(\cdot)$ is an indicator function. Thus, S ranges from 0 to 3. A *full-response* case was defined by $S = 3$, i.e., simultaneous improvement in all three performance indicators. Because equal weighting is a pragmatic simplification rather than an engineering optimum, score-based interpretation is used alongside the three continuous outcome metrics rather than in place of them.

A quartz/kaolinite ratio was then computed as an easily interpretable mineralogical screening index:

$$QK_i = \frac{\mathrm{Quartz}_i}{\mathrm{Kaolinite}_i}. \tag{5}$$

Statistical analysis

Because the number of additive-treated observations is modest ($n = 20$), robust non-parametric methods were used. Spearman rank correlation was employed to evaluate monotonic associations between raw descriptors and response metrics. Paired Wilcoxon signed-rank tests were used to compare perlite and tuff across the same ten clays. Mann–Whitney tests were used for group contrasts, and Fisher's exact test was used for the threshold-based full-response classification. Because each clay contributes two additive-treated observations that share the same mineralogical predictors, the primary observation-level analyses were complemented by three robustness checks: additive-specific subset analyses (perlite only and tuff only; $n = 10$ each), clay-level aggregation of response metrics across additives ($n = 10$), and leave-one-clay-out recalculation of the clay-level quartz/kaolinite–benefit relation. These checks were used to assess whether the ranking patterns persisted when the repeated-measures structure of the dataset was made more explicit. The analysis is therefore intentionally conservative and is interpreted as an exploratory deposit-screening framework rather than a universal predictive law.

RESULTS

Response heterogeneity at the 10 wt% *additive level*

Table 2 summarizes the additive response of each clay. Considerable heterogeneity is evident. Some clays improved in all three dimensions regardless of additive, whereas others exhibited trade-offs or outright deterioration in one or more outcomes. All three Hungarian clays (B, Y, G) achieved full response under both perlite and tuff. By contrast, SA6 showed adverse strength response with both additives, and SA7 improved strength only with tuff while losing density performance with both additives. The response spread across clays is therefore much larger than the difference between the two volcanic additives themselves.

At the mean level, perlite produced a slightly larger MHE gain (+9.3 percentage points vs. +8.1 for tuff), whereas tuff produced stronger average density reduction (−0.063 vs. −0.028 g/cm^3) and a larger mean UCS gain (+0.817 vs. +0.628 MPa). Nevertheless, additive identity was not the primary source of variation. Paired Wilcoxon tests detected no significant perlite–tuff difference for ΔMHE ($p = 0.539$), ΔBD ($p = 0.143$), or ΔUCS ($p = 0.770$). In other words, the dominant control at the selected dosage was not whether the additive was perlite or tuff, but how the raw clay interacted with either additive.

Table 2: Additive response metrics at the 10 wt% dosage relative to additive-free controls. Positive ΔMHE and ΔUCS are favorable; negative ΔBD is favorable. FullResp = 1 denotes simultaneous improvement in all three indicators.

Sample	Additive	ΔMHE	ΔBD (g/cm^3)	ΔUCS (MPa)	Score	FullResp
B	perlite	15	-0.04	0.26	3	1
B	tuff	19	-0.03	1.15	3	1
Y	perlite	11	-0.24	0.91	3	1
Y	tuff	3	-0.20	0.18	3	1
G	perlite	11	-0.02	0.41	3	1
G	tuff	16	-0.20	0.91	3	1
GZ1	perlite	14	-0.01	0.00	2	0
GZ1	tuff	1	-0.07	-0.12	2	0
FA2	perlite	15	-0.01	0.60	3	1
FA2	tuff	5	-0.03	3.98	3	1
SN3	perlite	15	-0.08	0.86	3	1
SN3	tuff	22	-0.05	-1.64	2	0
HL4	perlite	0	-0.01	1.20	2	0
HL4	tuff	-2	0.00	2.20	1	0
HL5	perlite	-4	-0.02	3.98	2	0
HL5	tuff	5	-0.09	1.36	3	1
SA6	perlite	0	0.06	-0.95	0	0
SA6	tuff	7	0.02	-1.05	1	0
SA7	perlite	16	0.09	-0.99	1	0
SA7	tuff	5	0.02	1.20	2	0

Figure 1 visualizes the magnitude and sign of the response metrics. Favorable cases cluster around the Hungarian clays and a small subset of Egyptian clays, underscoring that the central variability in the dataset is deposit-dependent rather than additive-dependent.

Quartz-rich, kaolinite-poor clays respond more favorably

The strongest mineralogical pattern concerned the quartz–kaolinite balance. Raw quartz correlated positively with the composite benefit score ($\rho = 0.773$, $p < 0.001$), while raw kaolinite correlated negatively ($\rho = -0.655$, $p = 0.002$). The density response was especially sensitive: quartz showed a strong negative association with ΔBD ($\rho = -0.728$, $p < 0.001$), whereas kaolinite showed a positive association ($\rho = 0.498$, $p = 0.025$), meaning that quartz-rich clays were more likely to become lighter after additive incorporation, while kaolinite-rich clays were more likely to remain unchanged or become denser. To test whether this pattern depended excessively on treating the 20 treated cases as independent, the ranking was re-examined in several ways. In additive-specific subsets, the quartz/kaolinite ratio remained positively associated with benefit score for both perlite ($\rho = 0.924$, $p < 0.001$) and tuff ($\rho = 0.665$, $p = 0.036$). When responses were averaged to one observation per clay, mean benefit score remained positively associated with raw quartz ($\rho = 0.850$, $p = 0.0019$) and quartz/kaolinite ($\rho = 0.887$, $p = 0.0006$) and negatively associated with raw kaolinite ($\rho = -0.755$, $p = 0.0115$). Leave-one-clay-out recalculations of the clay-level quartz/kaolinite–benefit relation remained uniformly positive ($\rho = 0.843$–0.927, all $p \leq 0.0043$). These internal validation checks do not remove the need for external replication, but they do indicate that the main mineralogical ranking is not an artifact of a single clay or of duplicated clay-level predictors.

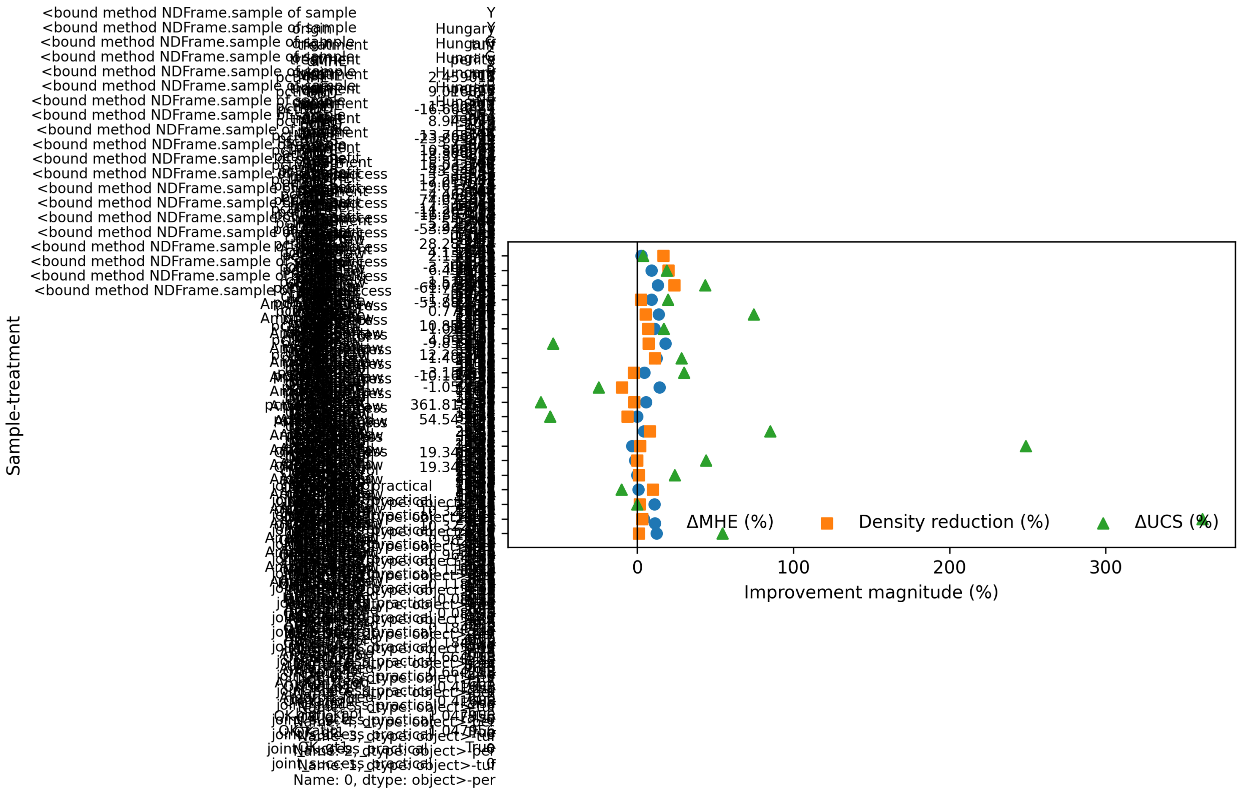

Figure 1: Improvement magnitudes for the additive-treated cases at 10 wt%. MHE and UCS are shown as percentage increases relative to the control; density reduction is plotted as a positive improvement quantity for ease of comparison.

Table 3 summarizes the observation-level correlation structure. Among the examined raw descriptors, the quartz/kaolinite ratio offered the clearest single predictor of multi-criteria benefit ($\rho = 0.799$, $p < 0.001$). By contrast, ΔUCS alone showed weaker dependence on quartz and kaolinite, indicating that density reduction is more composition-sensitive than strength increase. The robustness checks described above support the same ordering at the clay level, with somewhat stronger rank correlations after aggregation.

Table 3: Spearman correlations between raw-clay descriptors and additive response metrics across the 20 additive-treated observations. Significance levels: $^{*}p < 0.05$, $^{**}p < 0.01$, $^{***}p < 0.001$.

Predictor	ΔMHE	ΔBD	ΔUCS	Benefit score
Raw quartz	0.385	-0.728***	0.104	0.773***
Raw kaolinite	-0.338	0.498*	-0.077	-0.655**
Total flux	0.052	0.436	-0.450*	-0.336
Raw amorphous	-0.556*	-0.295	0.116	-0.047
Quartz/kaolinite	0.364	-0.683***	0.159	0.799***

Figure 2 maps the additive-treated cases in quartz–kaolinite space. Full-response observations cluster in the domain where quartz exceeds kaolinite, or where both minerals occur in near parity but quartz is not strongly subordinate. This reinforces the idea that the response is conditional, not universal.

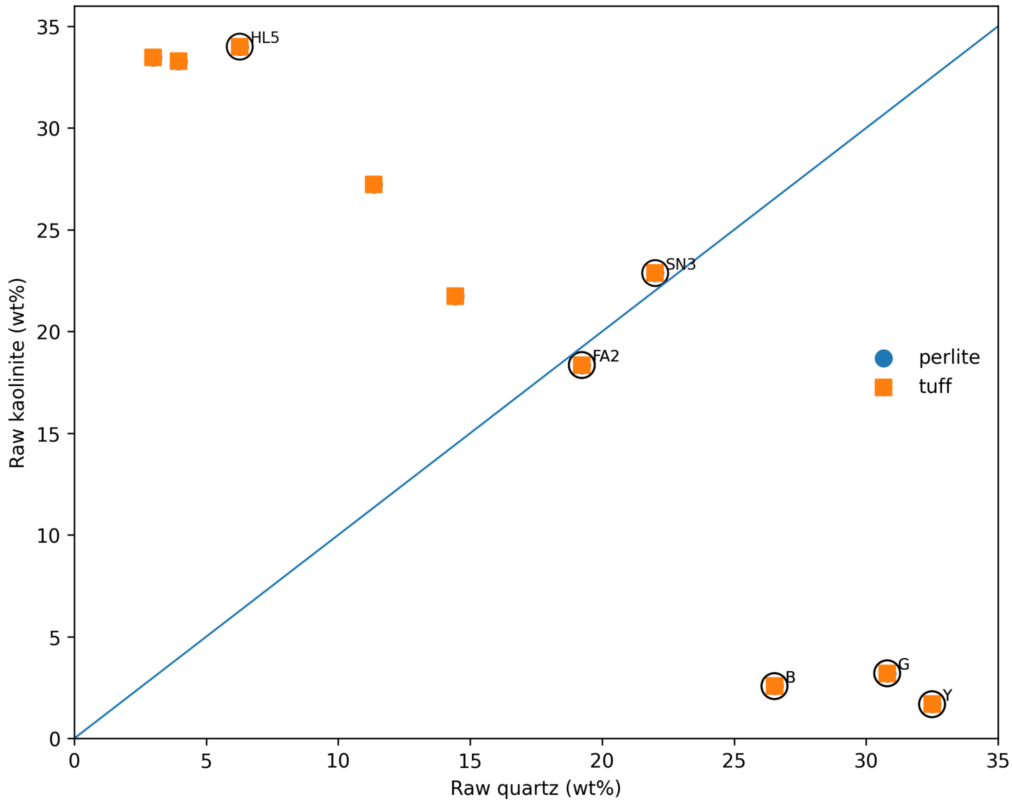

Figure 2: Raw quartz–kaolinite space for the additive-treated observations. Circled points denote full-response cases (simultaneous improvement in MHE, BD, and UCS). The diagonal line marks quartz = kaolinite.

Quartz/kaolinite ratio as a practical screening index

Within this dataset, the quartz/kaolinite ratio separated favorable and mixed responses with notable clarity. All eight additive-treated observations with $QK > 1$ achieved full response, whereas only 2 of 12 observations with $QK \leq 1$ did so (Fisher exact $p = 0.0007$). On average, the $QK > 1$ group attained a mean benefit score of 3.00 and a mean density reduction of $0.096\,\mathrm{g/cm^3}$; the $QK \leq 1$ group attained a mean benefit score of 1.75 and a mean density reduction of only $0.012\,\mathrm{g/cm^3}$. The difference in benefit score was significant ($p = 0.008$), as was the difference in full-response frequency ($p = 0.005$). The threshold pattern also persisted at the clay level: all four clays with $QK > 1$ achieved full response under both additives, whereas none of the six clays with $QK \leq 1$ did so (Fisher exact $p = 0.0048$).

Figure 3 presents this relation directly. The threshold does not imply a mechanistic discontinuity, but it does provide a practical rule-of-thumb for this dataset: when raw quartz is at least comparable to raw kaolinite, additive-assisted improvement is much more reliable at the 10 wt% dosage.

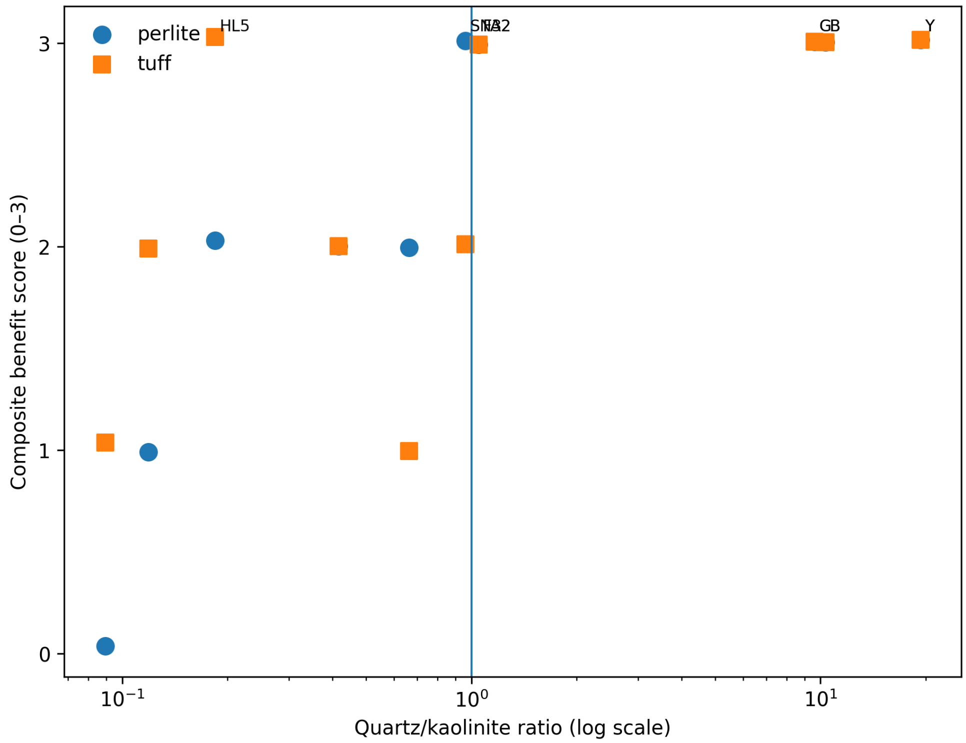

Figure 3: Quartz/kaolinite ratio versus composite benefit score for the additive-treated observations. The vertical line marks $QK = 1$. Full-response cases cluster to the right of this threshold.

Process–structure interpretation through the fired amorphous phase

The original experimental study reported that higher fired amorphous content is associated with lower density (Abdelfattah et al., 2023). The present analysis confirms that this relation is particularly strong in the additive-treated cases. For perlite-treated aggregates, the linear fit between fired amorphous content and BD yields $R^2 = 0.815$; for tuff-treated aggregates, $R^2 = 0.848$. These values are consistent with the trend reported in the source study and indicate that the downstream physical advantage of the more responsive clays is mediated by more effective glass-phase development and gas entrapment. Although direct viscosity measurements or time-resolved pore-evolution data were not available in the present re-analysis, the consistency of the amorphous–density relation across both additives supports the proposed process–structure interpretation.

The implication is important: raw mineralogy governs whether the additive helps the system move into a favorable viscous window, and the fired amorphous phase records the success of that transition. The mineralogical screening heuristic therefore aligns naturally with the process–structure–property pathway already implicit in the experimental observations.

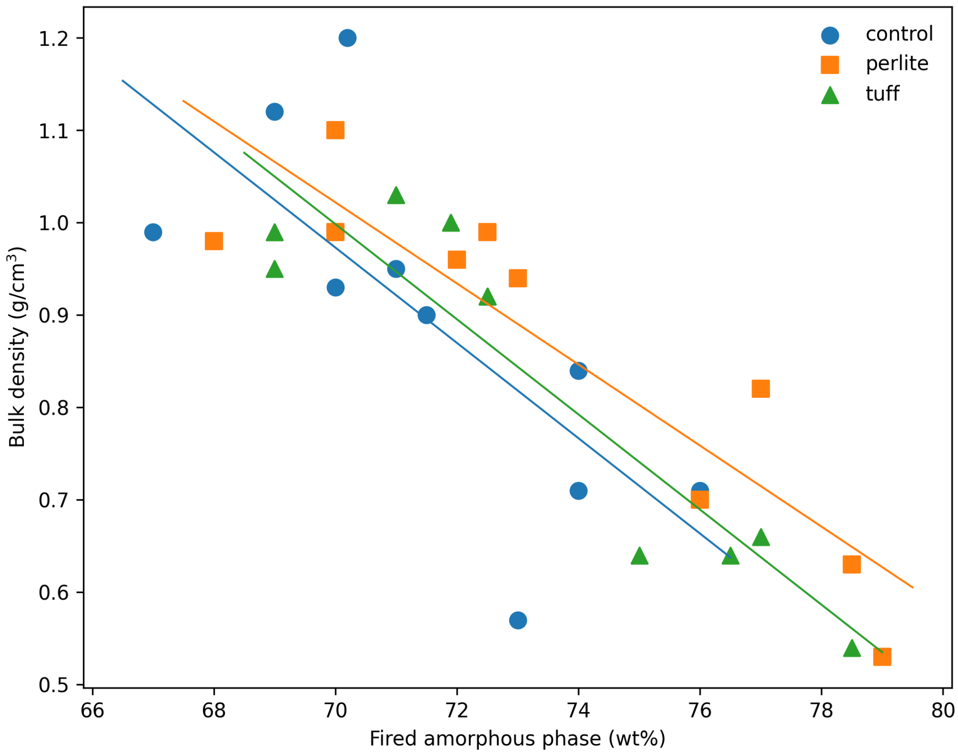

Figure 4: Bulk density as a function of fired amorphous content for control, perlite-treated, and tuff-treated aggregates. Additive-treated observations show a pronounced inverse relation between glass-phase abundance and density.

DISCUSSION

Why does kaolinite-rich clay behave differently?

The data suggest that the decisive issue is not overall silica abundance alone, but the balance between quartz-bearing framework components and kaolinite-rich clay fractions. In the source dataset, the more kaolinitic Egyptian clays frequently produced higher mullite proportions after firing, whereas the most responsive clays combined lower kaolinite with more favorable density reduction and more consistent full-response behavior (Abdelfattah et al., 2023). This does not mean quartz acts independently as the sole causal agent. Rather, the quartz/kaolinite ratio appears to serve as an empirical proxy for how the raw mineral mixture enters the bloating window under the selected firing schedules. The proposed mechanism should therefore be read as an interpretation anchored in phase assemblage trends, not as a fully isolated causal model.

At the temperatures used in the experimental program, kaolinite-rich systems are likely to favor more refractory transformation pathways, including stronger mullite development, while also requiring a more narrowly balanced viscosity to retain gas effectively. Under those conditions, a volcanic additive may still increase strength, but the density response becomes less reliable. That interpretation is consistent with the observation that ΔUCS alone was less strongly tied to quartz and kaolinite than ΔBD.

Implications for additive selection and process design

The practical implication is straightforward. Perlite and tuff are both viable, globally available volcanic additives (Abdelfattah et al., 2023; Dondi et al., 2004), and both can yield high-performing LWAs. Yet at the 10 wt% dosage, choosing the "better" additive in the abstract is less informative than first screening the clay. If XRD indicates that quartz is at least comparable to kaolinite ($QK > 1$), the probability of concurrent gains in MHE, BD, and UCS is high in this dataset. If $QK \leq 1$, pilot firing is still possible, but outcomes are more likely to involve trade-offs, especially for density. In practice, the criterion is best treated as a pre-screening aid that narrows the experimental search space, not as a substitute for confirmation firing.

This point is valuable for industrial workflows. XRD-based quartz and kaolinite quantification is faster and less expensive than repeated furnace trials across multiple additive dosages. A simple mineralogical screen can therefore reduce experimental burden and help prioritize clays for additive-assisted LWA production. The framework also complements modified Riley-type composition maps by introducing a mineral-phase-aware criterion rather than relying only on bulk oxide balance (Abdelfattah et al., 2023; Riley, 1951).

Scientific contribution relative to the existing literature

Previous studies have established that additives can alter expansion, density, compressive strength, and firing energy in clay-based LWAs (Bernhardt et al., 2014; Soltan et al., 2016; Wei et al., 2018). The present study contributes something different: it identifies a deposit-screening dimension that helps explain why the same additive can be highly effective for one clay and only partially effective for another. In that sense, the main advance is not a new additive, dosage, or firing route, but a mineralogical selection principle that converts a descriptive materials comparison into a testable screening framework. That distinction matters, because it positions the study as hypothesis-building and decision-support oriented rather than as a final predictive solution.

LIMITATIONS

Several limitations should be made explicit. First, the dataset contains ten clays and two additive-treated observations per clay, which is well suited to transparent non-parametric inference but not to high-dimensional predictive modeling. Although the observation-level analyses were supplemented by clay-level and leave-one-clay-out checks, the study still relies on a limited number of unique raw materials. Second, the inferential scope is tied to the 10 wt% dosage and to the firing temperatures selected in the experimental program; the proposed threshold should not be extrapolated automatically to other processing windows. Third, the work is a secondary analysis of reported measurements rather than a new laboratory campaign, so mechanistic interpretation remains constrained by the variables available in the source dataset. Fourth, the composite benefit score is intentionally simple and does not encode project-specific weighting among density, expansion, and strength. Fifth, the analysis is performed at the level of reported aggregate properties rather than raw image segmentation or pellet-by-pellet pore statistics. Future work should test whether the quartz/kaolinite threshold remains stable under broader raw-material libraries, additional dosages, direct image-derived pore metrics, and independent validation datasets.

CONCLUSIONS

A moderator-oriented examination of a ten-clay volcanic-additive matrix leads to the following conclusions:

1. Additive responsiveness is strongly clay-dependent. At the 10 wt% dosage, perlite and tuff produced full multi-criteria response in some clays and mixed or adverse response in others.
2. Raw mineralogy, rather than additive identity alone, is the dominant predictor of outcome within this dataset. Perlite and tuff showed no significant paired difference in ΔMHE, ΔBD, or ΔUCS.
3. Quartz-rich, kaolinite-poor clays respond most favorably. Raw quartz positively tracked the composite benefit score, while kaolinite tracked it negatively.
4. Density improvement is the most mineralogically sensitive outcome. Strong density reductions occurred primarily in clays with higher quartz and lower kaolinite.
5. A simple quartz/kaolinite ratio provides a practical screening heuristic. In this dataset, all additive-treated observations with $QK > 1$ achieved simultaneous improvement in expansion, density, and strength, and the same threshold pattern remained evident after aggregation to one observation per clay.
6. The screening rule is consistent with the process–structure pathway observed in the experimental program: favorable raw mineralogy promotes higher fired amorphous content, which in turn supports lower density through more effective gas retention.

Taken together, these findings provide a useful basis for pre-selecting clays for volcanic-additive modification before pilot-scale firing, thereby reducing experimental uncertainty and improving the targeting of lightweight aggregate feedstocks. At the same time, the proposed criterion should be regarded as a validated internal screening pattern within the present matrix, not as a replacement for broader experimental confirmation.

REFERENCES

Abdelfattah, M. M., Géber, R., & Kocserha, I. (2023). Enhancing the properties of lightweight aggregates using volcanic rock additive materials. *Journal of Building Engineering*, *63*, 105426. https://doi.org/10.1016/j.jobe.2022.105426

Agha, M. A., Ferrell, R. E., & Hart, G. F. (2012). Mineralogy of egyptian bentonitic clays. I: Discriminant function analysis. *Clays and Clay Minerals*, *60*, 387–404.

Bernhardt, M., Justness, H., Tellesbø, H., & Wiik, K. (2014). The effect of additives on the properties of lightweight aggregates produced from clay. *Cement and Concrete Composites*, *53*, 233–238. https://doi.org/10.1016/j.cemconcomp.2014.07.005

Dondi, M., Cappelletti, P., Cerri, G., de Gennaro, M., de Gennaro, R., & Langella, A. (2004). Zeolitic tuffs as raw materials for lightweight aggregates. *Applied Clay Science*, *25*, 71–81.

Gaber, M. A. W., & Hassanien, I. M. (2011). Applied geological studies of some sinai, egypt ore deposits to utilize as extender pigments for paint manufacture. *Advances in Petroleum Exploration and Development*, *1*(1), 66–77. https://doi.org/10.3968/j.aped.1925543820110101.008

Hossain, K. M. A. (2004). Properties of volcanic scoria based lightweight concrete. *Magazine of Concrete Research*, *56*(2), 111–120. https://doi.org/10.1680/macr.2004.56.2.111

Huang, C., & Liao, Y. (2011). Effects of heat treatment on the physical properties of lightweight aggregate from water reservoir sediment. *Ceramics International*, *37*, 3723–3730.

Hung, M. F., & Hwang, C. L. (2007). Study of fine sediments for making lightweight aggregate. *Waste Management & Research*, *25*(5), 449–456.

Pekgöz, M., & Tekin, K. (2021). Microstructural investigation and strength properties of structural lightweight concrete produced with zeolitic tuff aggregates. *Journal of Building Engineering*, *43*, 102863. https://doi.org/10.1016/j.jobe.2021.102863

Rashad, A. M. (2018). Lightweight expanded clay aggregate as a building material—an overview. *Construction and Building Materials*, *170*, 757–775. https://doi.org/10.1016/j.conbuildmat.2018.03.009

Riley, C. M. (1951). Relation of chemical properties to the bloating of clays. *Journal of the American Ceramic Society*, *34*(4), 121–128. https://doi.org/10.1111/j.1151-2916.1951.tb11619.x

Soltan, A. M. M., Kahl, W.-A., Abd El-Raoof, F., Abdel-Hamid El-Kaliouby, B., Abdel-Kader Serry, M., & Abdel-Kader, N. A. (2016). Lightweight aggregates from mixtures of granite wastes with clay. *Journal of Cleaner Production*, *117*, 139–149. https://doi.org/10.1016/j.jclepro.2016.01.017

Wei, Y., Weng, S., & Xie, X. (2018). Reduction of sintering energy by application of calcium fluoride as flux in lightweight aggregate sintering. *Construction and Building Materials*, *190*, 765–772. https://doi.org/10.1016/j.conbuildmat.2018.09.134

AUTOBIOGRAPHICAL SKETCHES

Dr. Zora Goodwin, University of Alaska; dgoodwin4@alaska.edu

Manuscript revisions completed 13 December 2023.